Forensic Science International 259 (2016) 246.e1–246.e5

Contents lists available at ScienceDirect

Forensic Science International

journal homepage: www.elsevier.com/locate/forsciint

Forensic Anthropology Population Data

Geometric morphometric analysis reveals sexual dimorphism in the distal femur

Etienne Cavaignac [a,b,*], Frederic Savall [a], Marie Faruch [a], Nicolas Reina [a,b], Philippe Chiron [b], Norbert Telmon [a]

[a] Laboratoire AMIS, UMR 5288 CNRS, Université Paul Sabatier, 37 allée Jules Guesdes, 31000 Toulouse, France
[b] Institut de l'appareil locomoteur, Hôpital Pierre-Paul Riquet, CHU Toulouse, France

ARTICLE INFO

Article history:
Received 26 May 2015
Received in revised form 23 September 2015
Accepted 8 December 2015
Available online 19 December 2015

Keywords:
Distal femur dimorphism
Principal component analysis
Procrustes analysis
Geometric morphometric analysis
Forensic anthropology population data

ABSTRACT

An individual's sex can be determined by the shape of their distal femur. The goal of this study was to show that differences in distal femur shape related to sexual dimorphism could be identified, visualized, and quantified using 3D geometric morphometric analysis.

Geometric morphometric analysis was carried out on CT scans of the distal femur of 256 subjects living in the south of France. Ten landmarks were defined on 3D reconstructions of the distal femur. Both traditional metric and geometric morphometric analyses were carried out on these bone reconstructions; these analyses identified trends in bone shape in sex-based subgroups.

Sex-related differences in shape were statistically significant. The subject's sex was correctly assigned in 77.3% of cases using geometric morphometric analysis.

This study has shown that geometric morphometric analysis of the distal femur is feasible and has revealed sexual dimorphism differences in this bone segment. This reliable, accurate method could be used for virtual autopsy and be used to perform diachronic and interethnic comparisons. Moreover, this study provides updated morphometric data for a modern population in the south of France.

2. Materials and methods

This was a retrospective descriptive analytical study. The research ethics committee at our healthcare facility approved this study (No. 01-0415).

The analysis was carried out on the CT images of 256 distal femurs residing in our facility's imaging database. Only scans showing the entire distal femur (tip of femoral groove to most distal aspect of femur) were retained. Any CT scans performed to assess disease conditions in the distal femur were excluded. The included CT scans had mainly been performed to assess leg vasculature (CT angiogram) or to evaluate a tibial plateau fracture. The CT scans were taken on a Sensation 16 Scanner (Siemens, Erlangen, Germany). Between June 1, 2014 and December 31, 2014, 256 CT scans of the distal femur met our inclusion criteria. There were 134 women and 122 men. The average age was 58 ± 15.2 years. The right side was analyzed 122 times and the left side 134 times. The groups were statistically similar (Table 1). The CT scans were saved as digital imaging and communications in medicine (DICOM) files and then processed with Amira 4.1.1® software (Mercury Computer System, Inc., Chelmsford, MA, USA).

Ten osteometric landmarks were defined based on standard bone landmarks used in anthropometry (Fig. 1 and Table 2) [4,11–13,24,25]. By using points typically associated with osteometric techniques, comparisons could be made with published studies on this subject to determine the plausibility of our results. The metric variables measured were the epicondylar breadth (EB), which is the distance between the two epicondyles [2,3,5–10,26], anterior posterior diameter of the medial condyle (APDMC), which is the largest anteroposterior dimension of the medial condyle [4,13], and anterior posterior diameter of the lateral condyle (APDLC), which is the largest anteroposterior dimension of the lateral condyle [4,13] (Fig. 2). All of these were Type I landmarks [21]. Once these landmarks had been located with 3D in vivo imaging software (Amira®, Visualization Sciences Group, Bordeaux, France), the coordinates of each landmark in space (x,y,z) were recorded.

* Corresponding author at: Institut de l'appareil locomoteur, Hôpital Pierre Paul Riquet, Place du Dr Baylac, TSA 40 031, 31059 Toulouse, France. Tel.: +33 60 07 342 595/561 775 582; fax: +33 561 322 232.
E-mail address: cavaignac.etienne@gmail.com (E. Cavaignac).

http://dx.doi.org/10.1016/j.forsciint.2015.12.010
0379-0738/

Table 1
Mean age of the various subgroups relative to sex and side. Comparisons were performed with Student's *t*-test.

		Age	*P*
Sex	Male ($n = 134$)	56.7 ± 14.42	0.445
	Female ($n = 122$)	58.14 ± 15.5	
Side	Right ($n = 122$)	57.36 ± 15.3	0.885
	Left ($n = 134$)	57.43 ± 14.7	

Table 2
Anatomical description of the various landmarks used, with the intra- and inter-observer variability for each. The error is given as a percentage.

Landmark	Location	Intra-observer variability	Inter-observer variability
1	Medial epicondyle	1.64	1.63
2	Most dorsal point on medial condyle	1.64	1.64
3	Top of intercondylar notch	1.64	1.64
4	Most dorsal point on lateral condyle	1.64	1.64
5	Lateral epicondyle	1.63	1.64
6	Most outside point on trochlear groove	1.63	1.65
7	Most distal point at bottom of trochlear groove	1.64	1.65
8	Most ventral point on margin of trochlear groove	1.64	1.65
9	Most distal point on medial condyle	1.53	1.51
10	Most distal point on lateral condyle	1.52	1.49

The analyzed data was taken from the same database and analyzed twice on separate occasions by two observers. This made it possible to calculate the intra- and inter-observer variability for each landmark. For each observer, landmark deviations were calculated relative to the landmark's mean value. The percentage error for each landmark was calculated, as described previously [32,34] (Table 2). The results were deemed acceptable if this error was less than 5% [32–35].

All morphometric geometric analyses were carried out with Morpho J software [27] and R 2.2.0 software [28]. The chosen landmarks made it possible to characterize the shape of the distal femur (Fig. 1). The first step consisted of a generalized Procrustes analysis (GPA) [20,29–31]. As described previously [19,20], this strategy expresses the results in graphical format by showing the average shape of the subgroups of interest.

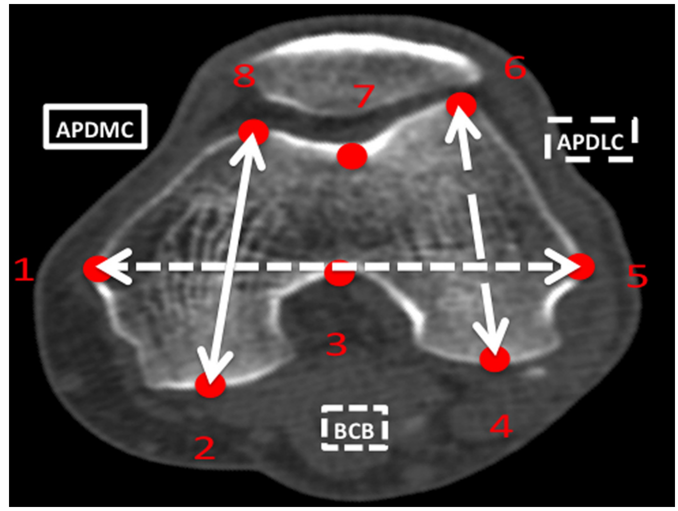

Fig. 2. Osteometric data used to measure the plausibility of the study's methodology. EB: epicondylar breadth, distance between the two epicondyles, APDMC: anterior posterior diameter of the medial condyle, which is largest anteroposterior dimension of the medial condyle [4,13] and APDLC: anterior posterior diameter of the lateral condyle, which is largest anteroposterior dimension of the lateral condyle [4,13].

The descriptive analysis consisted of calculating the mean, median and standard deviation values for each subgroup. A comparative analysis was performed with all the variables based on sex (male, female). The landmark coordinates were analyzed using principal component analysis (PCA) [30,31] and canonical variate analysis (CVA) to identify shape trends in the various subgroups [19,20].

A discriminant analysis was performed to determine the percentage of cases in which the sex was correctly estimated. Pearson's Chi-square test was used to determine if this analysis was statistically significant [30]. To determine if the difference between shapes was statistically significant, a *P*-value was also calculated using Goodall's *F*-test and Mahalanobis D2 matrices [36,37]. The length variables (EB, ADPLC and ADPMC) were compared using an analysis of variance (ANOVA).

3. Results

The percentage errors for the intra- and inter-observer comparisons for all the landmarks are given in Table 2. None

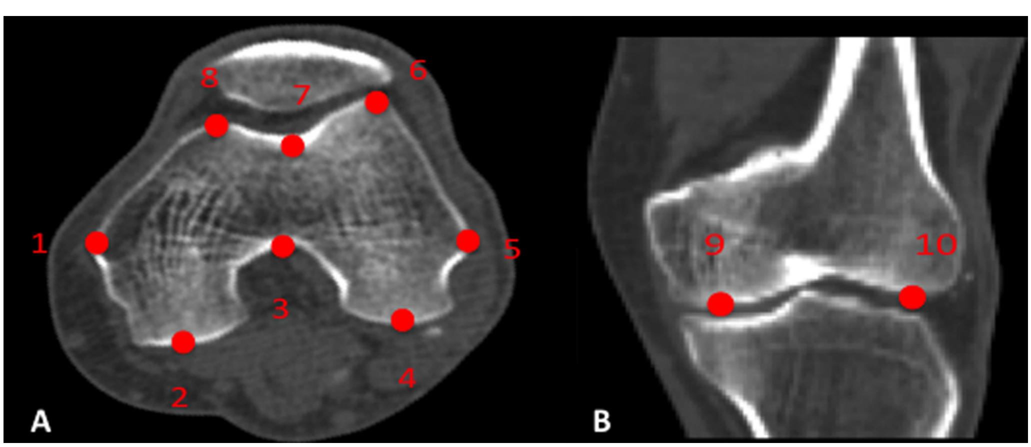

Fig. 1. Location of landmarks on axial (A) and frontal (B) CT scan slices: (1) medial epicondyle, (2) most dorsal point on medial condyle, (3) top of intercondylar notch, (4) most dorsal point on lateral condyle, (5) lateral epicondyle, (6) most ventral point on lateral edge of trochlear groove, (7) most distal point at bottom of the trochlear groove, (8) most ventral point on the medial edge of the trochlear groove, (9) most distal point on medial condyle, (10) most distal point on lateral condyle.